Journal of Cellular Biochemistry 104:2091–2106 (2008)

c-Myc Represses FOXO3a-Mediated Transcription of the Gene Encoding the p27^{Kip1} Cyclin Dependent Kinase Inhibitor

Vidyalakshmi Chandramohan,[1] Nora D. Mineva,[1] Brian Burke,[1] Sébastien Jeay,[1] Min Wu,[1] Jian Shen,[1] William Yang,[1] Stephen R. Hann,[2] and Gail E. Sonenshein[1]*

[1]Department of Biochemistry, Boston University Medical School, 715 Albany Street, Boston, Massachusetts 02118

[2]Department of Cell and Developmental Biology, Vanderbilt University School of Medicine, 1161 21st Ave South, Nashville, Tennessee 37221

Abstract The p27^{Kip1} (p27) cyclin-dependent kinase inhibitor and c-Myc oncoprotein play essential roles in control of cell cycle progression and apoptosis. Induction of *p27* (*CDKN1B*) gene transcription by Forkhead box O proteins such as FOXO3a leads to growth arrest and apoptosis. Previously, we observed that B cell receptor (surface IgM) engagement of WEHI 231 immature B lymphoma cells with an anti-IgM antibody results in activation of FOXO3a, growth arrest and apoptosis. As ectopic c-Myc expression in these cells prevented anti-IgM induction of *p27* and cell death, we hypothesized that c-Myc represses FOXO3a-mediated transcription. Here we show that c-Myc inhibits FOXO3a-mediated activation of the *p27* promoter in multiple cell lines. The mechanism of this repression was explored using a combination of co-immunoprecipitation, oligonucleotide precipitation, and chromatin immunoprecipitation experiments. The studies demonstrate a functional association of FOXO3a and c-Myc on a proximal Forkhead binding element in the *p27* promoter. This association involves the Myc box II domain of c-Myc and the N-terminal DNA-binding portion of FOXO3a. Analysis of publicly available microarray datasets showed an inverse pattern of c-*MYC* and *p27* RNA expression in primary acute myeloid leukemia, prostate cancer and tongue squamous cell carcinoma samples. The inhibition of FOXO3a-mediated activation of the *p27* gene by the high aberrant expression of c-Myc in many tumor cells likely contributes to their uncontrolled proliferation and invasive phenotype. J. Cell. Biochem. 104: 2091–2106, 2008.

Key words: FOXO3a; p27^{Kip1}; c-Myc; cancer

Forkhead box O (FOXO) transcription factors belong to the class of winged helix group of transcription factors. FOXO proteins have been implicated in the control of genes involved in multiple cellular processes, including cell cycle [Dijkers et al., 2000b; Medema et al., 2000], cell death [Brunet et al., 1999; Dijkers et al., 2000a], neoplastic transformation [Hu et al., 2004; Paik et al., 2007; Ticchioni et al., 2007], epithelial to mesenchymal transition [Belguise et al., 2007], longevity [Lin et al., 1997; Ogg et al., 1997], metabolism [Hall et al., 2000; Schmoll et al., 2000], and protection from oxidative stress [Kops et al., 2002; Nemoto and Finkel, 2002; Tothova et al., 2007]. There are three mammalian FOXO transcription factors, which are orthologues of *C. elegans daf-16*, FOXO1a, FOXO3a, and FOXO4. FOXO group members have an N-terminal DNA binding domain (Forkhead Domain), a nuclear localization signal (NLS), nuclear export signal (NES), and a C-terminal transactivation domain. FOXO factors function as transcriptional activators and bind as monomers to the consensus DNA sequence TTGTTTAC [Clark

This article contains supplementary material, which may be viewed at the Journal of Cellular Biochemistry website at http://www.interscience.wiley.com/jpages/0730-2312/suppmat/index.html.

Grant sponsor: NIH; Grant numbers: RO1 CA36355, PO1 ES11624, T32-AI07309.

*Correspondence to: Dr. Gail E. Sonenshein, Department of Biochemistry, Boston University School of Medicine, 715 Albany Street, Boston, MA 02118.
E-mail: gsonensh@bu.edu

Received 21 February 2008; Accepted 22 February 2008
DOI 10.1002/jcb.21765

et al., 1993; Kaufmann and Knochel, 1996; Furuyama et al., 2000]. Phosphorylation by Akt inhibits the activity of the FOXO proteins [Brunet et al., 1999; Hu et al., 2004]. Following phosphorylation on T32, S253 and S315, FOXO3a is bound by 14-3-3, and exported from the nucleus. Upon inhibition of Akt, activation of FOXO3a protein proceeds via de-phosphorylation and translocation into the nucleus where it induces transcription of target genes, including the *p27* (*CDKN1B* or *Kip1*) gene encoding the $p27^{Kip1}$ cyclin-dependent kinase inhibitor (CKI) [Dijkers et al., 2000b; Medema et al., 2000].

The p27 CKI, which mediates repression of cyclin E-CDK2 and cyclin A-CDK2 complexes leading to cell cycle arrest in G1, plays an essential role in control of cell cycle progression [Polyak et al., 1994], as well as the induction of apoptosis [Katayose et al., 1997; Wang et al., 1997; Wu et al., 1999]. For example, the induction of p27 levels in WEHI 231 immature B lymphoma cells results in G1/S phase arrest and apoptosis [Wu et al., 1999]. Many aggressive cancers are typified by decreased levels of p27 [Chiarle et al., 2001; Erlanson and Landberg, 2001], which is an independent prognostic factor in a broad spectrum of tumors. Consistently, *p27* knockout mice display a large mouse phenotype [Kiyokawa et al., 1996], as a result of an increase in cell number due, in part, to increased proliferation. The regulation of p27 is quite complex with control exerted at both transcriptional and post-transcriptional levels [Polyak et al., 1994; Kamesaki et al., 1998; Yang et al., 2001]. FOXO1a, FOXO3a, and FOXO4 have been found to transactivate the *p27* gene and to control cell cycle progression and apoptosis in various cell types [Dijkers et al., 2000b; Medema et al., 2000]. In addition, p27 activity is regulated at the levels of protein stability [Loda et al., 1997] and sequestration [Vlach et al., 1996].

Previously, we showed that ectopic expression of c-Myc reduces the induction of *p27* mRNA and protein levels associated with anti-IgM treatment of WEHI 231 B lymphoma cells [Yang et al., 2001]. Furthermore, we showed that overexpression of c-Myc inhibited the basal activity of the TATA-less *p27* promoter, in part, via binding to the +1 Inr region in Hs578T breast cancer cells, NIH 3T3 fibroblasts, and Jurkat T cells. Deletion of the Myc Box II (MBII) domain of c-Myc reduced the extent of inhibition of the *p27* promoter, as has been seen for other Inr-driven promoters [Li et al., 1994]. Since we have recently shown that anti-IgM treatment of WEHI 231 cells induces FOXO3a [Chandramohan et al., 2004], here we explored the hypothesis that activation of the *p27* promoter by FOXO3a is repressed via c-Myc. Our findings indicate that c-Myc inhibits FOXO3a-mediated activation of *p27* promoter via physical association, consistent with the inverse patterns of their expression seen in microarray analysis of a diverse group of human cancers.

MATERIALS AND METHODS

Cell Culture

WEHI 231 cells were maintained and treated with anti-μ (anti-IgM) heavy chain antibody at a concentration of 4 μg/ml as previously described [Wu et al., 1996]. NIH 3T3 fibroblasts, Hs578T breast cancer cells, Jurkat T cells and 293T human embryonic kidney cells were maintained, as described [Brunet et al., 1999; Izumi et al., 2001; Yang et al., 2001].

DNA Constructs

The *p27* promoter luciferase reporter constructs pλ34-11, ΔSstI, and ΔXhoI (see scheme in Supplementary Fig. 1A), and the ΔLZ-c-Myc and GST constructs were described elsewhere [FitzGerald et al., 1999; Yang et al., 2001]. The Mut3-pλ34-11 promoter construct was generated by introducing the Mut3, 3-bp mutation [5′-CGACTGCCCGCCACCTCCT-3′] into the −110 FOXO3a site [5′-CGACTGTTTGCCACCTCCT-3′] by site-directed mutagenesis using the QuickChange kit (Stratagene, La Jolla, CA). (The core of the element is underlined.) The different FOXO3a and c-Myc expression vectors used are described in detail in supplemental information.

Transfection Assays

Transient or stable transfections of WEHI 231 and Jurkat T cells were performed as we have described [Wu et al., 1996; Yang et al., 2001]. NIH 3T3 cells and Hs578T cells were transfected with FUGENE (Roche, Palo Alto, CA). Luciferase assays were performed and normalized, as we have described previously [Yang et al., 2001].

EMSA

The sequence of the WT *p27* −110 bp oligonucleotide is 5′-CGCTCCGACTGTTTGC-

CACCTCCTCCT-3′, where the core Forkhead element is underlined. The sequences of the WT and mutant *p27* + 1 oligonucleotides are: 5′-CCTGCGCCTCTCTTCCCCAGACCTGCGCGCTACTGCGG-3′; 5′-CCTGCGCCTCTCTTCCCCAGACGGGGGGGCTACTGCGG-3′. WEHI 231 nuclear extracts and GST and GST fusion proteins were prepared from bacterial lysates and used in EMSA, as described previously [FitzGerald et al., 1999; Yang et al., 2001].

Immunoblotting and Immunoprecipitation

Whole cell extracts (WCEs) were prepared for immunoblotting or co-immunoprecipitation (co-IP) using Triton lysis buffer as described previously [Brunet et al., 1999]. Nuclear proteins were isolated as described [Wu et al., 1996]. Samples were removed for analysis of input (5%) and for co-IP (400–500 μg). Co-IPs were performed as described [Brunet et al., 1999], using antibodies against FOXO3a (06-951; Upstate, Lake Placid, NY), c-Myc [Wu et al., 1996], or V5 epitope (R960-25; Invitrogen, Carlsbad, CA). Cell extracts and purified immune complexes were separated on 8% polyacrylamide (PAGE)–SDS gels, for 2 or 2 h 50′, respectively, and immunoblotted as described [Wu et al., 1996].

Biotinylated Oligonucleotide Precipitation Assay

Cultures of 293T or NIH 3T3 cells at 50–60% confluence were transiently transfected using GenePORTER™ 2 transfection reagent (Genlantis, San Diego, CA) and oligonucleotide precipitation (ONP) assay was performed as described in Supplemental Information.

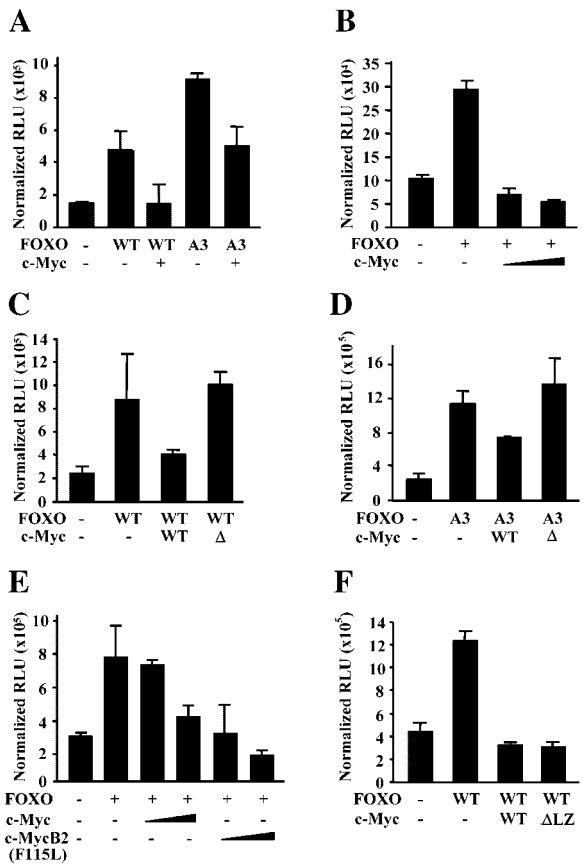

Fig. 1. c-Myc represses the induction of *p27* by FOXO3a, through its MBII domain. **A**: NIH 3T3 cells were transfected, in triplicate, with 1 μg pλ34-11 *p27* promoter-luciferase reporter construct, 1 μg either pECE (−FOXO) or pECE-FOXO3a WT (WT) or pECE-A3 FOXO3a (A3) in the presence of 1 μg either pRC (−c-Myc) or pRC-Myc (+c-Myc) DNA, and 0.25 μg of SV40-β-gal. Cells were harvested after 48 h and extracts normalized for equal amounts of β-gal activity, assayed and average values of luciferase activity are presented ±SD. The luciferase assay was performed at least three different times with similar results. Immunoblotting confirmed equal expression of WT and A3 FOXO3a proteins (data not shown). **B**: Hs578T breast cancer cells were transfected in triplicate with 1 μg pλ34-11 *p27*, 1 μg of either pcDNA3 (−FOXO) or pcDNA3-FOXO3a (+FOXO) in the presence of 0.5 or 1.0 μg pCsF-c-Myc (increasing c-Myc) or pCsF DNA (−c-Myc) and 0.5 μg SV40-β-gal. Cells were processed as above, and the average ± SD presented. The luciferase assay was performed two times with similar results. **C**,**D**: NIH 3T3 cells were transfected with 1 μg *p27* pλ34-11 in the presence or absence of 1 μg WT FOXO3a (C) or A3 FOXO3a mutant (D) expression vector and 1 μg MLV-Myc (WT) or MLV-Myc dlMBII (Δ) and enough empty vector (EV) DNA to make the final amount 3 μg. Extracts were prepared at 48 h, and luciferase activity, normalized for protein amount, presented as the average ±SD. The luciferase assay was performed three times with similar results. Immunoblotting confirmed equal expression of WT and dlMBII c-Myc (data not shown). **E**: Jurkat T cells were electroporated with 10 μg pλ34-11 *p27* plus 10 μg pECE-FOXO3a WT vector DNA, in the presence of either 10 μg pMLV (−c-Myc), or of either 5 or 10 μg pMLV-Myc or pMLV-MycB2 vector, expressing either WT or c-Myc F115L mutant, respectively, and enough EV DNA to make a total amount of 10 μg DNA per sample. Alternatively, cells were electroporated with 10 μg pλ34-11 plus 10 μg EV DNA (−). In addition, 5 μg SV40-β-gal was added, to normalize for transfection efficiency. Cells were harvested and processed as above and the average ± SD presented. The luciferase assay was performed three times with similar results. **F**: Jurkat T cells were electroporated, in triplicate, with 15 μg pλ34-11 plus 10 μg pECE-FOXO3a WT vector DNA, in the absence or presence of either 10 μg EV DNA (−Myc), or 10 μg pcEFL-Myc or pcEFL-Myc ΔLZ vectors, expressing WT or c-Myc LZ deletion mutant, respectively, plus 5 μg SV40-β-gal vector DNA to normalize for transfection efficiency. Cells were harvested after overnight incubation, and results are presented as average luciferase activity normalized for β-gal activity ±SD. The luciferase assay was performed three different times with similar results. Immunoblot analysis confirmed equal levels of c-Myc expression by these vectors (data not shown).

RNA Analysis

Cytoplasmic RNA was isolated from WEHI 231 cells and analyzed as previously described [Schauer et al., 1996] using a *cad* cDNA (kindly provided by Peggy Farnham, University of Wisconsin-Madison Medical School, WI), and *gapdh*, as loading control, as probe.

Chromatin Immunoprecipitation Assay

WEHI 231 cells were either left untreated or treated with anti-μ heavy chain antibody at a concentration of 4 μg/ml for 2, 4, or 8 h and then fixed with 1% formaldehyde. Chromatin immunoprecipitation (ChIP) assays were performed as described in Supplemental Information.

Gene Expression Analysis

The following microarray datasets of primary human cancers were accessed using the ONCOMINE™ Cancer Profiling Database (www.oncomine.org): Andersson_Leukemia (reporter number IMAGE:812965/IMAGE:854668) [Andersson et al., 2007]; Lapointe_Prostate (reporter number IMAGE:417226/IMAGE:627509) [Lapointe et al., 2004]; Talbot_Lung (reporter number 37724_at/2034_s_at) [Talbot et al., 2005]. Box plots, depicting the distribution of c-*MYC* or *p27* RNA expression within each group, and *P* values by Student's *t*-test for the comparison of the groups were obtained directly through the Oncomine 3.0 software. The line within the box represents the median expression value for each group, and the upper and lower edges of the box indicate the 75th and 25th percentile of the distribution, respectively. The lines (whiskers) emerging from each box extend to the smallest and largest observations; the black dots outside the ends of the whiskers are outlier data points.

RESULTS

p27 Promoter Activation by FOXO3a Is Inhibited by c-Myc

To test the hypothesis that c-Myc represses transactivation of the *p27* promoter by FOXO3a, NIH 3T3 cells were transiently transfected with the *p27* pλ34-11 promoter construct plus vectors expressing either WT FOXO3a (pECE-HA-FOXO3a) or a constitutively active mutant FOXO3a (A3 FOXO3a), in which three sites of Akt phosphorylation (T32, S253, S315) have been mutated to alanine residues, in the absence or presence of WT c-Myc expression vector (Fig. 1A). Co-expression of c-Myc completely ablated the induction of the *p27* promoter by WT FOXO3a (Fig. 1A). A3 FOXO3a showed a greater ability to induce *p27* promoter activity (6.2 vs. 3.2-fold), consistent with its inability to be phosphorylated by Akt and thereby exported from the nucleus. Co-transfection of a c-Myc expression vector reduced transactivation of the *p27* promoter by A3 FOXO3a by ~2.5-fold (Fig. 1A). Similarly, inhibition of FOXO3a-mediated activation of *p27* promoter activity was seen in Hs578T breast cancer cells (Fig. 1B). Thus, c-Myc inhibits promoter activation by FOXO3a.

Inhibition by c-Myc Is Mediated Via the MBII Domain

We next sought to identify the regions involved in inhibition by c-Myc. Given the critical role of the MBII domain in repression by c-Myc [Li et al., 1994], vectors expressing WT c-Myc or MBII deleted c-Myc (Δ) were co-transfected with either WT FOXO3a (Fig. 1C) or A3 FOXO3a (Fig. 1D) and the pλ34-11 *p27* promoter construct. Strikingly, c-Myc with MBII deletion was completely unable to prevent the activation of the *p27* promoter by WT FOXO3a or A3 FOXO3a, in contrast to the effects of WT c-Myc. The mutation of phenylalanine 115 in c-Myc to leucine (F115L) within the MBII region occurs in various Burkitt's lymphomas [Yano et al., 1993], and increases the ability of c-Myc to transform [Lee et al., 1996]. Using limiting doses of WT c-Myc or c-MycB2 (F115L c-Myc) vectors (Fig. 1E), expressing equal levels of Myc protein [Yang et al., 2001], it was observed that the mutation in the MBII domain of c-Myc enhanced its ability to repress activation of the *p27* promoter by FOXO3a. A c-Myc mutant with deletion of the leucine zipper region ΔLZ-c-Myc was also tested. The ΔLZ-c-Myc reduced FOXO3a-mediated activation of the *p27* promoter in transient co-transfection analysis to an extent essentially comparable to WT c-Myc (Fig. 1F), excluding the requirement for the LZ domain of c-Myc in this inhibition. Thus, the MBII domain of c-Myc is required for c-Myc to inhibit the induction of the *p27* promoter by FOXO3a.

The N-Terminal DNA Binding Domain of FOXO3a Mediates Association With c-Myc

To test for physical association of FOXO3a and c-Myc, co-IP assays were performed. Cells

were co-transfected with vectors expressing WT FOXO3a (V5 tagged) and WT c-Myc or ΔLZ-c-Myc, or parental empty vector (EV) DNA, as control. WCEs were subjected to co-IP with a c-Myc antibody followed by western blotting for the V5 tag. FOXO3a protein was detected with both the WT and ΔLZ-c-Myc but not with the EV control (Fig. 2A). Conversely, IP with a V5 antibody followed by immunoblotting for c-Myc detected both WT c-Myc and ΔLZ-c-Myc (Fig. 2B), confirming the ability of FOXO3a and c-Myc to associate.

Next, we tested the ability of endogenous FOXO3a and c-Myc to interact in WEHI 231 cells, a model well characterized with respect to expression of these proteins [Yang et al., 2001; Chandramohan et al., 2004]. In particular, anti-IgM treatment causes a transient increase in the levels of c-Myc protein at 2 h, which then declines below baseline; c-Myc resides predominantly in the nucleus at all times [Maheswaran et al., 1991]. Total FOXO3a levels are essentially equivalent in control and 8 h anti-IgM treated cells, however, most of the FOXO3a protein is localized in the cytoplasm during exponential growth, and moves to the nucleus following an 8 h treatment [Chandramohan et al., 2004]. Co-IP analysis was performed with WCEs prepared from control and 8 h anti-IgM-treated WEHI 231 cells. When extracts from untreated WEHI 231 cells were used, the antibody for FOXO3a brought down a low level of c-Myc, whereas, after 8 h of anti-IgM treatment, high levels of c-Myc co-precipitated (Fig. 2C). In

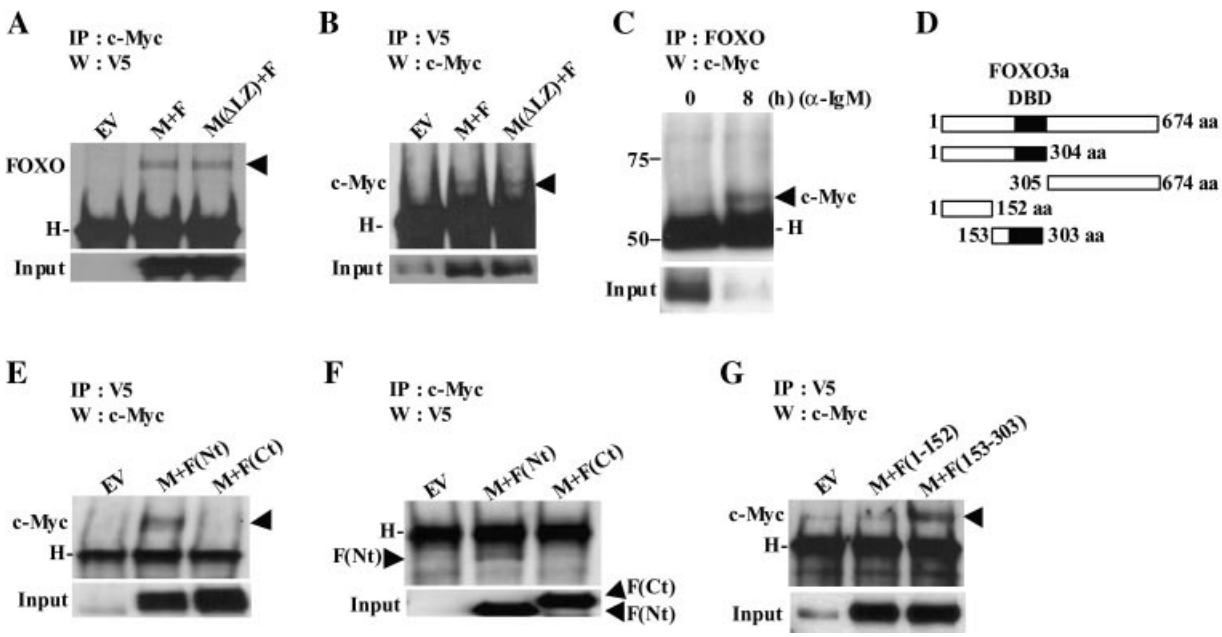

Fig. 2. c-Myc interacts with FOXO3a. **A**,**B**: WCEs (400 μg) were prepared from NIH 3T3 cells transfected with 3 μg of pcDNA4-FOXO3a-V5 (F) plus 3 μg of either pcEFL-Myc (M) or pcEFL-Myc ΔLZ [M(ΔLZ)] vectors, expressing WT or c-Myc LZ deletion mutant. Alternatively, cells were transfected with equivalent amounts of the appropriate EV. WCEs were subjected to IP either with (A) c-Myc antibody, and precipitated proteins analyzed by immunoblot with V5 antibody or (B) an antibody against the V5 tag and precipitated proteins analyzed by immunoblot with c-Myc antibody. As control for input, 5% of the WCEs were used. H—IgG heavy chain. **C**: WCEs (500 μg) prepared from WEHI 231 cells either left untreated (0) or treated with anti-IgM for 8 h were subjected to IP with FOXO3a antibody and precipitated proteins analyzed by immunoblot with c-Myc antibody. As control for input, 5% of the WCEs were used. H—IgG heavy chain. **D**: Schematic representation of FOXO3a full length and deletion constructs. DBD, DNA binding domain. **E**,**F**: WCEs (400 μg) were prepared from NIH 3T3 cells transfected with 5 μg of either pcDNA3.1-FOXO3a-Nt-V5 (V5 tagged, N-terminal 1-304 amino acid FOXO3a) [F(Nt)] or pcDNA3.1-FOXO3a-Ct-V5 (V5 tagged, C-terminal 305-674 amino acid FOXO3a) [F(Ct)] along with 5 μg of FLAG-c-Myc expression vector (M) or with EV alone. WCEs were subjected to IP either with (E) an antibody against the V5 tag and precipitated proteins analyzed by immunoblot with c-Myc antibody or (F) c-Myc antibody, and precipitated proteins analyzed by immunoblot with V5 antibody. As control for input, 5% of the WCEs were used. H—IgG heavy chain. **G**: WCEs (400 μg) were prepared from NIH 3T3 cells transfected with 3 μg of either pcDNA4-FOXO3a-1-152-V5 (V5 tagged, N-terminal 1-152 amino acid FOXO3a) [F(1-152)] or pcDNA4-FOXO3a-153-303-V5 (V5 tagged, N-terminal 153-303 amino acid FOXO3a) [F(153-303)] along with 3 μg of FLAG-c-Myc expression vector (M) or with EV alone. WCEs were subjected to IP with an antibody against the V5 tag and precipitated proteins analyzed by immunoblot with c-Myc antibody. As control for input, 5% of the WCEs were used. H—IgG heavy chain.

contrast, no enhanced binding was seen when rabbit IgG was used (data not shown). Thus, endogenous FOXO3a and c-Myc associate following movement of FOXO3a to the nucleus after 8 h of anti-IgM treatment despite a substantial decrease in overall levels of c-Myc (see input c-Myc levels, bottom panel in Fig. 2C).

To identify the regions of FOXO3a responsible for interaction with c-Myc, constructs that express either the N-terminal 1-304 amino acids of FOXO3a (pcDNA3.1-FOXO3a-Nt-V5), containing the DNA binding domain, or the C-terminal 305–674 amino acids (pcDNA3.1-FOXO3a-Ct-V5), containing the transactivation domain, were used (see Fig. 2D). IP with an antibody against the V5 tag followed by western blotting for c-Myc demonstrated that the N-terminal and not the C-terminal region of FOXO3a interacts with c-Myc (Fig. 2E), which was confirmed in the reciprocal co-IP analysis (Fig. 2F). The N-terminal region of FOXO3a was further divided into two fragments comprising amino acids 1–152 or 153–303 of FOXO3a (Fig. 2D). As seen in Figure 2G, the c-Myc binding site localized to the amino-terminal residues 153–303. Thus, the region containing the DNA binding domain of FOXO3a mediates association with c-Myc.

A Proximal Forkhead Binding Site Maps at −110 bp of the *p27* Promoter

To map the elements mediating activation of the *p27* promoter in WEHI 231 cells, transfection analysis was performed using a series of *p27* promoter deletion constructs (Supplementary Fig. 1A). Anti-IgM treatment induced the two larger pλ34-11 and ΔSstI constructs approximately 3.2- and 2.4-fold, respectively, while the activity of the shorter ΔXhoI *p27* promoter construct was unaffected (Supplementary Fig. 1B). Thus, most of the activation can be mapped to the −45 to −342 bp promoter region. In addition, a second element appears to be located further upstream, between −342 and −2002 bp, consistent with the mapping of Medema et al. [2000].

Using TFSearch and 80% homology, a putative Forkhead factor binding site was localized at −110 bp of the *p27* promoter (Fig. 3A). Since a FOXO3a supershifting antibody is not currently available, bacterially expressed glutathione-S-transferase (GST)-FOXO3a fusion protein was used in EMSA with an oligonucleotide containing this element (termed −110 *p27*). GST-FOXO3a protein bound to the −110 *p27* oligonucleotide in EMSA, yielding two major complexes (Fig. 3B), while control GST protein failed to bind (The GST-FOXO3a protein preparation yielded two bands in SDS–PAGE (data not shown), suggesting partial clipping or synthesis, consistent with the findings of Brunet et al. [1999]). Successful competition with excess unlabeled −110 *p27* element, or an oligonucleotide containing the FOXO3a site of the *IGFBP1* promoter, termed IRS [Brunet et al., 1999], indicated the specificity of the binding (Fig. 3B). The identity of the Forkhead element was further confirmed in ONP assays. Specifically, purified GST-FOXO3a, and not control GST proteins, bound well to a biotinylated oligonucleotide probe containing the WT −110 *p27* sequence, but not to ones containing either a Mut3 or Mut6 sequence (Fig. 3C). Furthermore, robust binding to the WT probe was seen with ectopically expressed FOXO3a protein in NIH 3T3 cells (Fig. 3D). FOXO3a binding to the −110 *p27* promoter element was also demonstrated using extracts prepared from NIH 3T3 cells transfected with a vector expressing an ERα tagged FOXO3a protein (pcDNA3-HA-FOXO3a:ER) versus EV pcDNA3 DNA following treatment with 500 nM tamoxifen (4-OHT) (Supplementary Fig. 1C). Consistently, a dose-dependent increase in p27 levels and nuclear expression of HA-FOXO3a:ER were seen with 4-OHT treatment (Supplementary Fig. 1D). HA-FOXO3a:ER binding could be competed with the WT but not Mut3 or Mut6 oligonucleotides (data not shown). Lastly, the effects of introducing Mut3 into the pλ34-11 promoter construct were assessed. The WT promoter construct was induced in a dose-dependent fashion by pcDNA3-FOXO3a to a substantially higher level than the Mut3-pλ34-11 promoter construct (Supplementary Fig. 1E), consistent with deletion of the functional proximal element. Taken together, these studies identify a functional Forkhead binding site within the −110 bp region of the *p27* promoter.

c-Myc Associates With FOXO3a Bound to the −110 *p27* Promoter Element

Given that repression by c-Myc can involve interaction with positive regulating factors [Izumi et al., 2001], the hypothesis that c-Myc

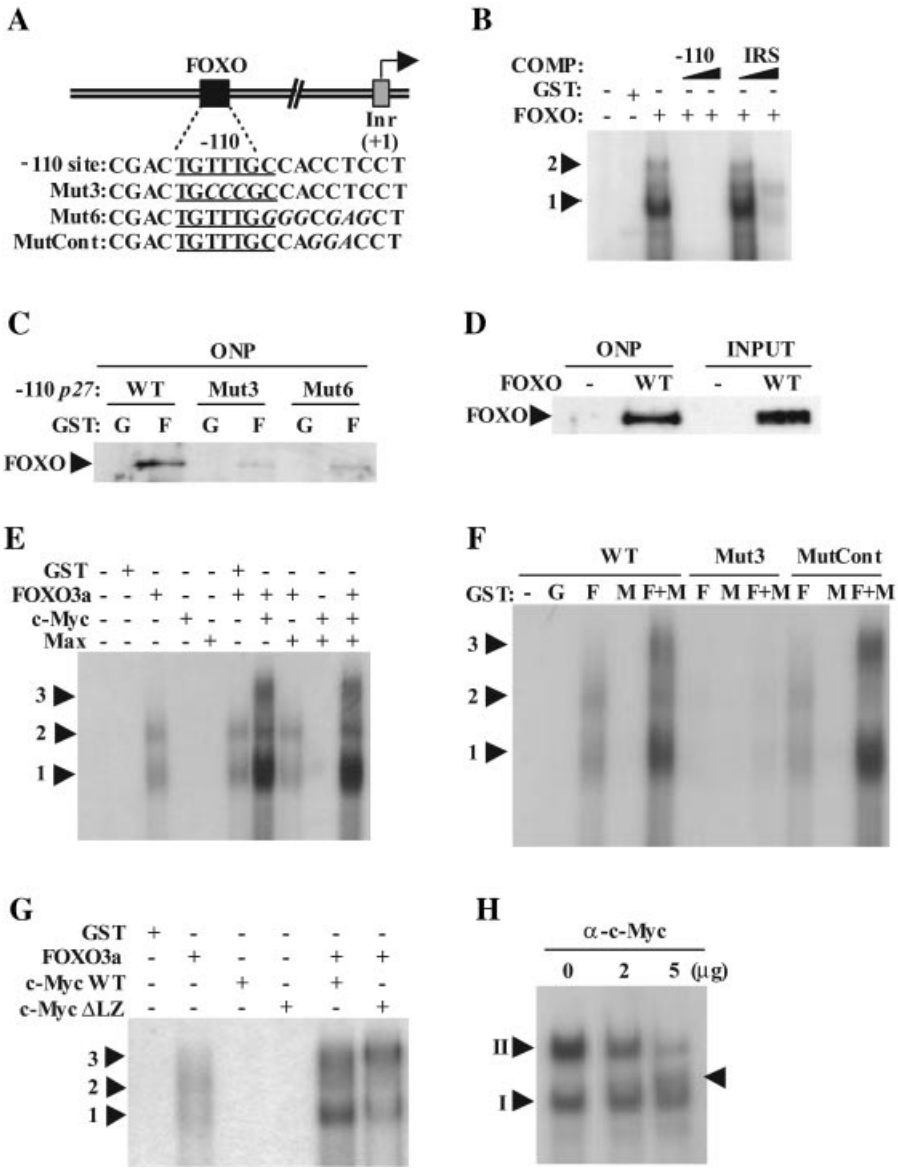

Fig. 3. FOXO3a binding to the −110 bp *p27* promoter Forkhead element facilitates c-Myc binding. **A**: Scheme of the *p27* promoter with WT and mutant versions of the −110 bp putative Forkhead site. The core of the element is underlined, and the mutations are given in italics. **B**: Either 300 ng GST-FOXO3a fusion protein or GST protein alone, as control, was used in EMSA with the −110 *p27* oligonucleotide, as probe. For competition experiments (COMP), 50× or 200× molar excess of either −110 *p27* or IRS Forkhead unlabeled oligonucleotide was added to the binding mixture. Shown is a representative EMSA of three independent experiments. **C**: Six hundred nanogram GST-FOXO3a (F) or GST (G) alone were subjected to ONP assays using either 5′ biotinylated −110 *p27* WT, Mut3 or Mut6 oligonucleotide as probe, and assessed for precipitated FOXO3a protein. Shown is a representative blot of three independent experiments. **D**: WCEs were prepared from NIH 3T3 cells transfected with 5 μg HA-FOXO3a or EV DNA. Samples (250 μg) were subjected to ONP assay using −110 *p27* WT oligonucleotide, as probe. The precipitated complexes and 4% of the WCEs, used as control for input, were subjected to immunoblot analysis with a FOXO3a antibody. Shown is a representative blot of three independent experiments. **E**: EMSA was performed using 300 ng GST-FOXO3a and GST-c-Myc, or 150 ng GST-Max or GST alone, as indicated, with labeled −110 *p27* WT oligonucleotide as probe. The complexes observed are termed bands 1, 2, and 3. Shown is a representative EMSA of three independent experiments. **F**: Three hundred nanogram GST-FOXO3a (F) and GST-c-Myc (M) protein, or 150 ng of GST protein (G) alone were used, as indicated, with labeled −110 *p27* WT, Mut3 and MutCont oligonucleotides as probes. Shown is a representative EMSA of three independent experiments. **G**: EMSA was performed using 300 ng GST-FOXO3a and GST-c-Myc, and GST-c-Myc ΔLZ, or GST alone, as indicated, in binding reactions with labeled −110 *p27* WT oligonucleotide, as probe. The complexes observed were termed bands 1, 2, and 3. Shown is a representative EMSA of two independent experiments. **H**: Nuclear extracts (10 μg) from WEHI 231 cells treated with anti-IgM for 4 h were incubated overnight at 4°C in the absence (0) or presence of 2 or 5 μg of c-Myc antibody (α-c-Myc), prior to EMSA with labeled −110 *p27* WT oligonucleotide as probe. The complexes observed were termed bands I and II. Arrowhead, position of new band that appears following removal of bound c-Myc with addition of antibody. Shown is a representative EMSA of two independent experiments.

can be recruited to the WT −110 *p27* oligonucleotide by FOXO3a was tested in EMSA (Fig. 3E). Addition of GST-FOXO3a plus GST-c-Myc yielded a new slower migrating complex (band 3) in addition to the two complexes (bands 1 and 2) observed with GST-FOXO3a alone; furthermore, the intensity of band 1 increased substantially (Fig. 3E). GST, or GST-c-Myc and GST-Max proteins added alone or in combination failed to bind; furthermore, addition of GST-Max did not have a discernable effect on complex formation by FOXO3a and c-Myc. The requirement for the Forkhead element was confirmed when the Mut3 oligonucleotide with a 3 bp mutation in the Forkhead element was used. GST-FOXO3a was unable to bind, and only a very low level of binding was seen with GST-c-Myc plus GST-FOXO3a (Fig. 3F). In contrast, complex formation appeared essentially unaffected by a 3 bp mutation in a downstream region (MutCont) (Fig. 3F). EMSA confirmed GST-ΔLZ-c-Myc can interact with GST-FOXO3a bound to the −110 bp *p27* oligonucleotide (Fig. 3G), consistent with the observed ability of ΔLZ c-Myc to interact with and inhibit FOXO3a-mediated transactivation of the *p27* promoter. Together, these results indicate c-Myc can interact with FOXO3a protein bound to its element within the −110 *p27* region.

When nuclear extracts prepared from WEHI 231 cells following anti-IgM treatment were used in EMSA with the WT −110 *p27* oligonucleotide as probe, a profile of low basal binding of two bands (I and II) at 0 h was seen to increase substantially at 4 and 8 h post-anti-IgM treatment (data not shown), consistent with the activation of nuclear FOXO3a [Chandramohan et al., 2004], and increased *p27* mRNA levels [Yang et al., 2001]. To assess for the presence of c-Myc, the 4 h-time point of anti-IgM treatment was selected since c-Myc levels have not yet decreased below basal values at this time point [Wu et al., 1996], and an increase in FOXO3a binding was noted [Chandramohan et al., 2004]. Incubation of WEHI 231 nuclear extracts with 2 μg of c-Myc antibody reduced formation of the upper complex (band II), while 5 μg anti-c-Myc almost totally inhibited the binding of the upper complex, and resulted in the appearance of an additional band, which migrated near the lower complex (Fig. 3H). Overall, the results are consistent with band II containing c-Myc likely in a complex with FOXO3a, and band I likely consisting of FOXO3a, which normally binds as a monomer [Clark et al., 1993].

FOXO3a Mediates c-Myc Binding to the *p27* Promoter

Previously, c-Myc repression of the *p27* promoter activity was shown to be mediated via binding to the +1 Inr region in a complex with Max [Yang et al., 2001]. To test for DNA–protein interaction, ONP assays were performed using WCEs from cells transfected with HA-FOXO3a or FLAG-c-Myc expression vectors alone or in combination or with EV DNA, as control and either WT or Mut3 −110 *p27* oligonucleotide as probe (Fig. 4A,B). c-Myc was unable to bind to the WT −110 *p27* promoter region when expressed by itself, but was able to bind when co-expressed with FOXO3a (Fig. 4A). Binding of c-Myc was greatly decreased when the Mut3 oligonucleotide was used (Fig. 4B). The c-Myc protein with MBII deletion (Δ) was unable to bind to the WT −110 *p27* element in the presence of WT FOXO3a (Fig. 4C), indicating the involvement of the MBII domain in the association of c-Myc with FOXO3a. As an additional control, binding to the +1 region was assessed since c-Myc/Max interaction does not depend upon the MBII domain. A low level of c-Myc binding to the +1 *p27* WT oligonucleotide was seen in the absence of co-transfected Max, as expected given the ubiquitous expression of Max, and binding was enhanced by ectopic Max expression (Fig. 4D). A mutated version of the +1 *p27* region, unable to bind Max or c-Myc proteins in EMSA [Yang et al., 2001], displayed greatly reduced c-Myc binding (Fig. 4E). Of note, the binding profile of c-Myc protein with a deletion of MBII to the WT +1 region was essentially identical to that with the WT c-Myc protein: low level in the absence of Max, which increased upon expression of Max (Fig. 4F). Therefore, the MBII domain does not appear to be required for binding via the +1 region. Strikingly, we noted that expression of FOXO3a had an opposite effect on binding of c-Myc to the +1 *p27* element. FOXO3a reduced binding of WT c-Myc to the +1 *p27* region (Fig. 4D), in contrast to findings with the WT −110 *p27* element. The observation that MBII deleted c-Myc binding to the +1 *p27* region was unaffected by FOXO3a (Fig. 4F), suggested that this may be due to direct interactions. Taken together, these results indicate c-Myc (via its MBII domain) can bind to FOXO3a on the −110

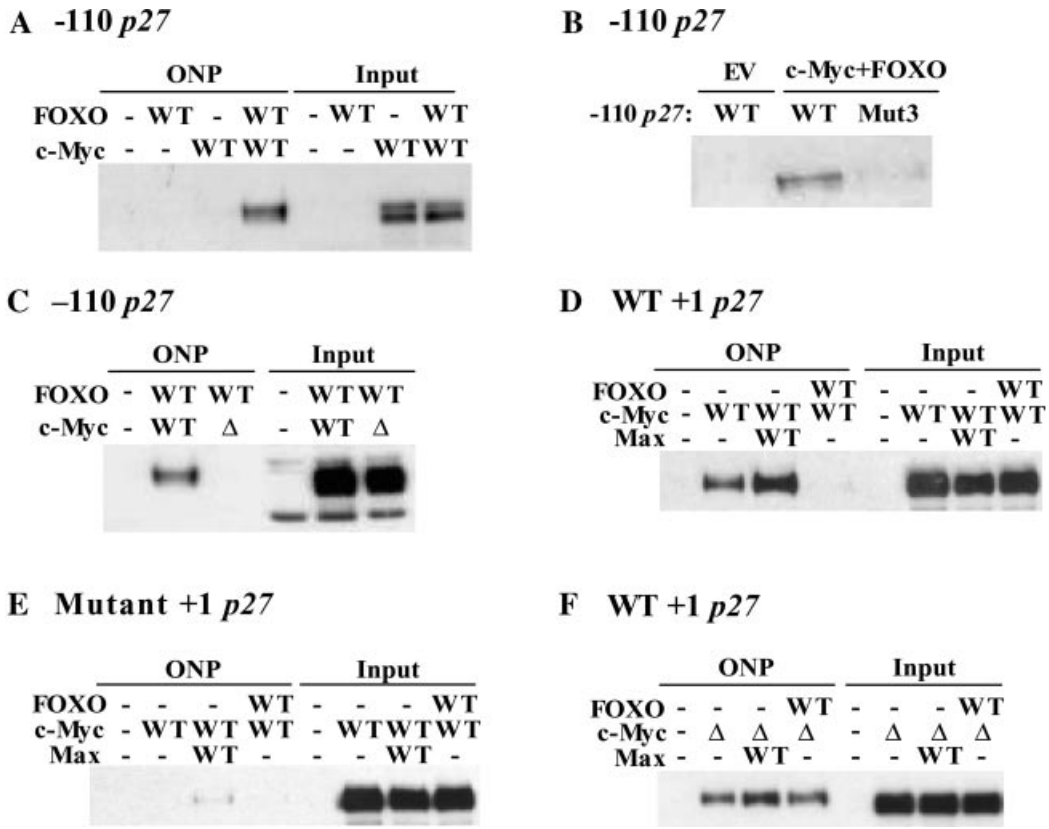

Fig. 4. The MBII domain of c-Myc is required for its interaction with FOXO3a at the −110 *p27* region. **A**: WCEs were prepared from 293T cells transfected with 5 μg HA-FOXO3a and 5 μg FLAG-c-Myc expression vectors either alone or in combination, or with EV alone (−). Samples (600 μg) were subjected to ONP assays using biotinylated −110 *p27* WT oligonucleotide as probe, or 3% of the WCE was used as control for input. The precipitated complexes were subjected to immunoblotting analysis with an anti-FLAG antibody to assess c-Myc levels. Shown is a representative blot of three independent experiments. **B**: WCEs (600 μg) from 293T cells transfected with either 5 μg FLAG-c-Myc and 5 μg HA-FOXO3a expression vectors or EV DNA were subjected to ONP using either −110 *p27* WT or Mut3 oligonucleotide as probe, as above. Shown is a representative blot of two independent experiments. **C**: WCEs (600 μg) from 293T cells transfected with 5 μg of either FLAG-c-Myc (WT) or FLAG-c-Myc-Δ129-145, expressing deletion MBII FLAG-c-Myc (Δ), in the presence of 5 μg of WT HA-FOXO3a expression vectors, or EV, as indicated, were subjected to ONP using −110 *p27* WT oligonucleotide, and immunoblotted for FLAG protein. Alternatively, 3% of the WCE was used as control for input. Shown is a representative blot of two independent experiments. **D–F**: WCEs were prepared from NIH 3T3 cells transfected with 4 μg vector expressing WT or deletion MBII FLAG-cMyc (Δ), Max, HA-FOXO3a, or appropriate EV (−) as indicated. Samples (600 μg) were subjected to ONP assays using as probe either (D,F) WT +1 *p27* oligonucleotide, or (E) Mutant +1 *p27* oligonucleotide. Alternatively 3% of the WCE was used as control for input. The precipitated complexes were subjected to immunoblot analysis with an anti-FLAG antibody to assess c-Myc levels. Shown is a representative blot of two independent experiments.

p27 promoter region, whereas, activation of FOXO3a levels reduces c-Myc binding to the +1 region.

Promoter Occupancy Shifts From c-Myc to FOXO3a During Induction of *p27* Gene Expression

To assess the in vivo binding of these factors to the *p27* promoter region, we next used ChIP assays, although, the close proximity of the +1 and −110 bp elements precludes distinction between these two binding sites. Asynchronously growing WEHI 231 cells (0 h) were subjected to anti-IgM treatment for 2 h, which leads to an initial decrease in *p27* transcription, or for 8 h, which induces *p27* transcription [Ezhevsky et al., 1996; Wu et al., 1999]. The level of c-Myc binding to the *p27* promoter region in untreated WEHI 231 cells (Fig. 5A, upper panel), increased 2 h post-anti-IgM treatment, and then decreased at 8 h (Fig. 5A). Max binding also increased at 2 h and decreased at

8 h (Fig. 5A), although, the levels of Max protein remain constant with anti-IgM treatment out to this time (data not shown). The parallel changes in binding of c-Myc and Max are consistent with the fact that these two partners bind to the Inr region together [Yang et al., 2001].

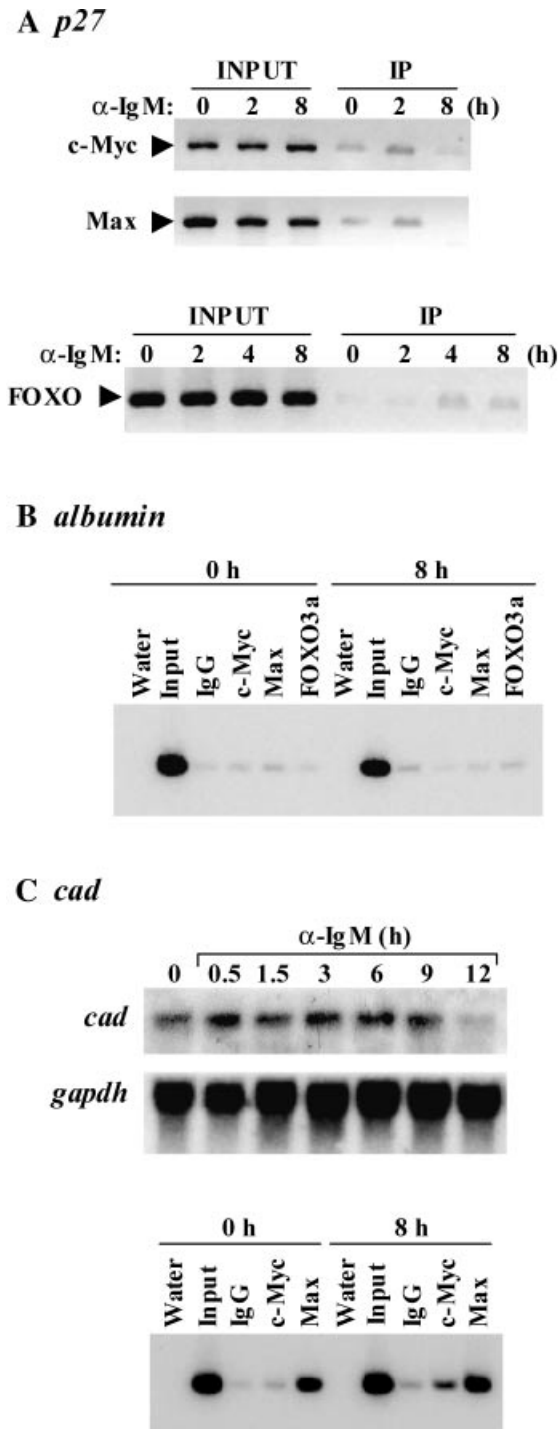

We next investigated FOXO3a binding at the *p27* promoter in WEHI 231 cells treated for 0, 2, 4, or 8 h with anti-IgM (Fig. 5A, lower panel). FOXO3a levels on the *p27* promoter were low during asynchronous growth and up to 2 h of anti-IgM treatment. After 4 h, an increase in binding was noted, which was sustained out to 8 h (Fig. 5A), consistent with the kinetics of changes in *p27* mRNA levels following anti-IgM treatment [Wu et al., 1999]. As a negative control for the binding, the promoter for *albumin*, which is not expressed in these B cells, was similarly assayed by ChIP. No binding was detected with this promoter, confirming the specificity of binding to the *p27* promoter (Fig. 5B). As a positive control for c-Myc binding, we similarly assessed carbamoylphosphate synthase (glutamine-hydrolyzing)/aspartate carbamoyltransferase/dihydroorotase (*cad*), an E-box containing gene that is positively regulated by binding of c-Myc with its partner Max [Eberhardy et al., 2000]. The effects of anti-IgM on the profile of *cad* expression in WEHI 231 cells were examined first. The expression of *cad* mRNA increased by 0.5 h of anti-IgM treatment and then remained essentially constant until 9 h (Fig. 5C, upper panel). Between 9 and 12 h, *cad* mRNA levels decreased substantially. Analysis of *gapdh*

Fig. 5. *p27* promoter occupancy changes from c-Myc/Max to FOXO3a during anti-IgM-induced apoptosis of WEHI 231 cells. **A**: WEHI 231 cells were in asynchronous growth (0 h) or treated with anti-IgM (α-IgM) for 2, 4, or 8 h, as indicated. Cells were formaldehyde crosslinked, sonicated, and subjected to immunoprecipitation using antibodies against (**upper panel**) c-Myc or Max, or (**lower panel**) FOXO3a. The precipitated DNA and input samples were amplified by PCR using primers specific for the *p27* promoter and analyzed on 1% agarose gels. Shown is a representative ChIP of two independent experiments. **B**: Asynchronously growing WEHI 231 cells (0 h) were treated with anti-IgM for 8 h. Samples were immunoprecipitated using control IgG, or antibodies against c-Myc, Max, or FOXO3a and amplified using primers specific for the *albumin* promoter. Alternatively, water was similarly analyzed. Shown is a representative ChIP of three independent experiments. **C** (**upper panel**): WEHI 231 cells were in asynchronous growth (0 h) or treated with anti-IgM for 0.5, 1.5, 3, 6, 9, or 12 h, as indicated. RNA was isolated and subjected to Northern blot analysis for mRNA levels of *cad* and *gapdh*, which confirmed loading was essentially equal. Shown is a representative of two independent experiments. C (**lower panel**): Asynchronously growing WEHI 231 cells (0 h) were treated with anti-IgM for 8 h. Samples were immunoprecipitated using control IgG, or antibodies against c-Myc or Max, and amplified using primers specific for the E-box region of the *cad* promoter. Alternatively, water was similarly analyzed. Shown is a representative ChIP of three independent experiments.

mRNA confirmed essentially equal loading. ChIP assays of the *cad* promoter indicated that the c-Myc and Max binding to the E-box remained detectable out to 8 h (Fig. 5C, bottom panel), in contrast to the findings with the *p27* promoter. Thus, high levels of c-Myc binding are seen when *p27* promoter activity is low, while elevated FOXO3a and reduced c-Myc and Max binding correlate with the induction of *p27* promoter activity following anti-IgM treatment.

Levels of *p27* and c-*MYC* Transcripts Vary Inversely in Human Cancer

Next, the ONCOMINE™ Cancer Profiling Database was searched to determine whether the predicted inverse relationship exists between the expression of the *p27* and c-*MYC* genes in human cancers. As seen on the box plots presented in Figures 6A–C (top panels), c-*MYC* expression was significantly increased (P values < 0.05) in acute myeloid leukemia, prostate cancer, and tongue squamous cell carcinoma patient samples as compared to their corresponding controls, consistent with its role in promoting these malignancies. The expression of *p27* was also evaluated in these same studies, which revealed a significant decrease in *p27* mRNA levels in the cancer versus normal samples in all three studies (Fig. 6A–C, lower panels). Thus, consistent with the observations that c-Myc inhibits *p27* activation by FOXO3a, an inverse correlation between *p27* and c-*MYC* mRNA levels exists in many primary tumor specimens.

DISCUSSION

Here we show for the first time that c-Myc inhibits FOXO3a-mediated activation of the *p27* promoter. These findings are consistent with the inverse pattern of expression of *p27* and c-*MYC* observed in acute myeloid leukemia, prostate cancer and tongue squamous cell carcinoma, and with the previous observation that ectopic c-Myc prevents induction of endogenous p27 protein expression following activation of FOXO3a in anti-IgM-treated WEHI 231 cells [Chandramohan et al., 2004]. Importantly, c-Myc was able to associate with FOXO3a at the proximal Forkhead element on the *p27* promoter; although, our data cannot distinguish between indirect association versus direct interaction. This association requires the MBII domain of c-Myc, which has been implicated in the ability of c-Myc to function as a repressor of gene transcription [Li et al., 1994], including the *p27* gene [Yang et al., 2001]. The N-terminal 153–303 amino acids of FOXO3a, which contain the DNA binding domain, are essential for this interaction. It should be noted that the possibility exists that another factor plays a role in FOXO3a/c-Myc interaction in vivo, in particular given the mobility of the complex seen upon addition of the c-Myc antibody with nuclear extracts from WEHI 231 cells. Thus, our data indicate repression of the *p27* gene transcription by c-Myc is mediated via binding at two sites (−110 and +1 bp) and is facilitated by two different factors FOXO3a (Forkhead element dependent) and Max (Inr element dependent), respectively (see models in Fig. 6D,E). Overall, these findings argue for a critical role of c-Myc in negative regulation of transcriptional activation by FOXO3a.

The PI3K to Akt signaling pathway, which is activated in many cancers, plays reciprocal roles in the regulation of FOXO3a and c-*Myc* gene expression. Phosphorylation of FOXO3a by Akt leads to its inactivation via sequestration in the cytoplasm [Brunet et al., 1999]. The PI3K to Akt pathway negatively controls the level of p27 expression in WEHI 231 cells [Chandramohan et al., 2004]. In contrast, PI3K/Akt signaling activates NF-κB, which induces c-*Myc* gene transcription in many cell types, including WEHI 231 B cells [Lee et al., 1995; Arsura et al., 2000; Grumont et al., 2002]. Thus, the high Akt activity that typifies many cancers leads to increased c-Myc levels and reduced nuclear FOXO3a. Furthermore, gene amplification, rearrangement, or point mutations in the c-*MYC* gene are quite common in cancer, leading to either constitutive overexpression of WT c-Myc [Lee et al., 1996], or expression of a mutant form, for example, F115L which functions as a super repressor protein. The high c-Myc activity mediates a decrease in p27 that could promote proliferation and cancer (Fig. 6D). Consistently, low p27 levels have been associated with a more invasive phenotype in many cancer, including of the breast and prostate [Catzavelos et al., 1997; Tsihlias et al., 1998]. Conversely, as cells normally approach quiescence, Akt activity is reduced. As a result, the levels of nuclear FOXO3a would

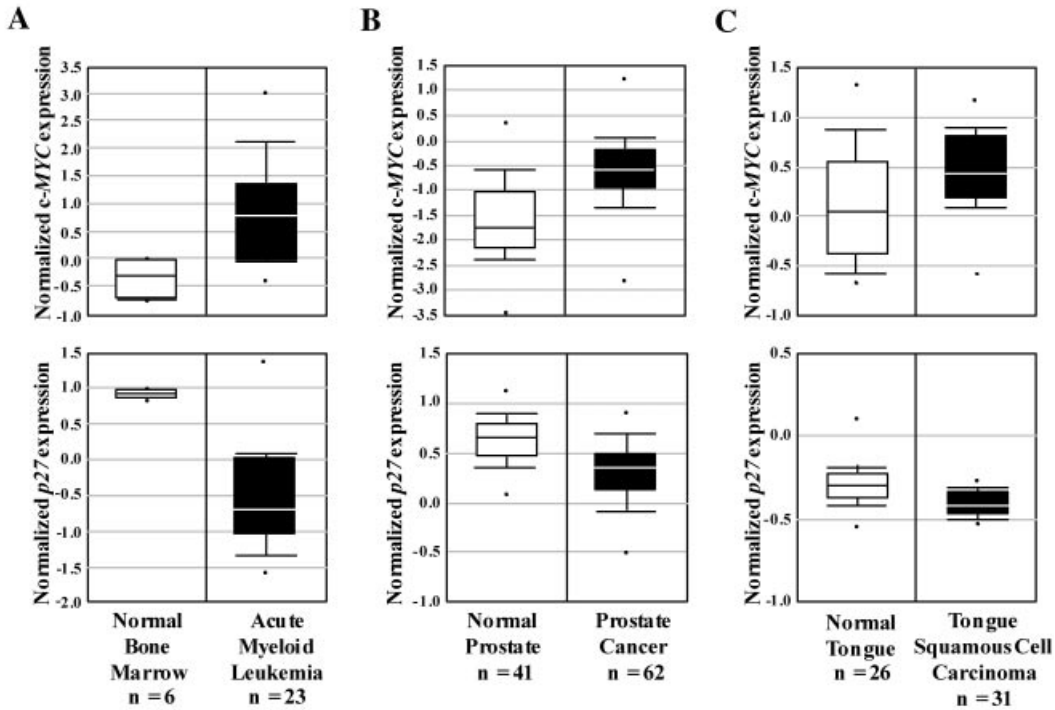
A
B
C
Normalized c-MYC expression
Normalized p27 expression
Normal Bone Marrow n = 6
Acute Myeloid Leukemia n = 23
Normal Prostate n = 41
Prostate Cancer n = 62
Normal Tongue n = 26
Tongue Squamous Cell Carcinoma n = 31

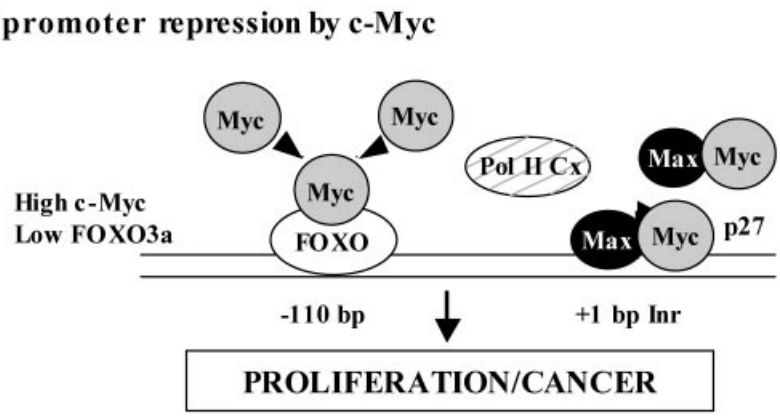
D p27 promoter repression by c-Myc
Myc
Myc
Myc
Pol II Cx
Max
Myc
High c-Myc
Low FOXO3a
FOXO
Max
Myc
p27
-110 bp
+1 bp Inr
PROLIFERATION/CANCER

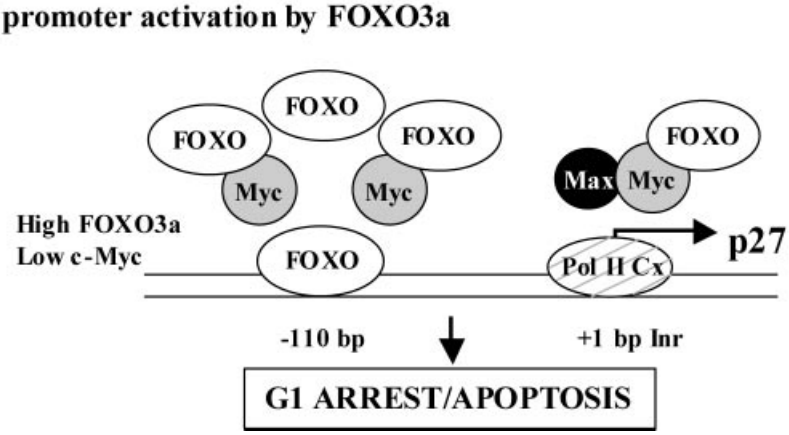
E p27 promoter activation by FOXO3a
FOXO
FOXO
FOXO
FOXO
Max
Myc
Myc
Myc
High FOXO3a
Low c-Myc
FOXO
Pol II Cx
p27
-110 bp
+1 bp Inr
G1 ARREST/APOPTOSIS

Fig. 6.

be increased and those of c-Myc decreased. The resulting excess nuclear FOXO3a protein can bind to the −110 bp proximal and distal Forkhead sites, and possibly titrate c-Myc/Max complexes away from the +1 Inr site. Thus, c-Myc–FOXO3a interactions may play an additional role in release of repression, thereby allowing for the activation of *p27* gene transcription leading to growth arrest (Fig. 6E).

Since the work of Roeder and coworkers first implicated c-Myc in repression of Inr-driven transcription [Roy et al., 1993], multiple mechanisms have been elucidated, which have many similarities to the regulation of *p27*. Activation of the PDGF-β-receptor by NF-Y could be repressed by c-Myc and required the MBII domain, and binding of NF-Y was not inhibited by c-Myc [Izumi et al., 2001]. The induction of $p15^{INK4b}$ by TGF-β1 was shown to involve upstream binding of Smad2/3 proteins [Seoane et al., 2001]. Repression by c-Myc in this case was mediated via direct interaction of c-Myc with the Smad2/3 activating complex [Feng et al., 2002], as well as binding of c-Myc, Max, and Miz-1 to the +1 Inr element [Staller et al., 2001], although, the functional role of Max binding was not examined. Lastly, c-Myc has been found to interfere with transactivation of the *p21* promoter mediated by Sp1, which binds at a site near to the +1 element [Claassen and Hann, 2000; Gartel et al., 2001]. Consistent with the findings of Penn, Farnham and coworkers showing an essential role of Max in repression by c-Myc [Mao et al., 2003; Barsyte-Lovejoy et al., 2004], transfection and gel shift analysis indicated an important role of c-Myc/Max binding at the +1 Inr region in repression of the *p27* promoter [Yang et al., 2001]. Importantly, ChIP assays have confirmed the transient induction and then drop of c-Myc and Max binding and the delayed binding of FOXO3a to the *p27* promoter in the anti-IgM treated WEHI 231 cells (Fig. 5); although, binding to the −110 bp and the +1 Inr could not be distinguished due to their proximity.

Here, we observed that the N-terminal Forkhead domain of FOXO3a mediates its association with c-Myc. Similarly, Seoane and coworkers demonstrated that the N-terminal DNA binding domain within amino acid region 139–280 of FOXO3a is involved in its interaction with Smad3/4, which in turn controls the activation of the $p21^{Cip1/Waf1}$ promoter [Seoane et al., 2004]. Furthermore, Smad and FOXO3a form an additional complex with FOXG1, a transcriptional repressor belonging to the Forkhead family leading to the repression of the $p21^{Cip1/Waf1}$ promoter [Seoane et al., 2004]. Here and in the studies by Bouchard et al. [2004], the reciprocal functional regulation of c-Myc and FOXO factors has been shown specifically with FOXO3a. Overall, the interactions between c-Myc and FOXO3a, which require the MBII domain of c-Myc and DNA binding region of FOXO3a, regulate activation by FOXO3a. Of note, transcription of several other genes is controlled by FOXO3a and c-Myc, including *ERα*, *bim*, and *gadd45* [Dijkers et al., 2000a; Tran et al., 2002]. Given the ability of FOXO3a and c-Myc to physically associate and for this association to affect DNA binding and thereby their activities, it is of importance to evaluate the role of these interactions in the transcriptional control of these genes.

ACKNOWLEDGMENTS

We thank B. Burgering, M. Greenberg, C. Dang, L. Freedman, M. Cole, M. Deckert, E. Ziff, and P. Farnham for generously providing cloned DNAs and antibodies. We gratefully acknowledge Anne Brunet, Randy Strough, and Shangqin Guo for helpful comments and suggestions. We thank Paloma H. Giangrande and Wencheng Zhu for generously providing assistance with the ChIP assays. This work was

Fig. 6. Inverse relationship between expression of *p27* and c-*MYC* transcripts in human cancer. **A–C**: Box plots showing levels of c-*MYC* (**upper panels**) or *p27* (**lower panels**) in primary normal versus cancer patient samples accessed through the ONCOMINE™ Cancer Profiling Database. A: Andersson_Leukemia Study: *P*-value for c-*MYC* comparison equals $3.2e^{-5}$, *P*-value for *p27* comparison equals $3.1e^{-10}$ [Andersson et al., 2007]. B: Lapointe_Prostate Study: *P*-value for c-*MYC* comparison equals $1.2e^{-8}$, *P*-value for *p27* comparison equals $3.6e^{-8}$ [Lapointe et al., 2004]. C: Talbot_Lung Study: *P*-value for c-*MYC* comparison equals 0.004, *P*-value for *p27* comparison equals $2.3e^{-4}$ [Talbot et al., 2005]. The number of samples (n) in each set is indicated below box plots. **D,E**: Schematic models of the roles of c-Myc and FOXO3a in repression and activation of the *p27* promoter. Relatively high levels of c-Myc (Myc) lead to repression of *p27* promoter activity and reduced p27 levels (as seen in highly proliferating cells and in cancer) (D), whereas elevated FOXO3a promotes increased p27 expression, as seen in cells undergoing growth arrest or apoptosis (E).

supported by grants from the NIH RO1 CA36355 (G.E.S.) and PO1 ES11624 (G.E.S.), and training grant T32-AI07309 (B.B.).

REFERENCES

Andersson A, Ritz C, Lindgren D, Eden P, Lassen C, Heldrup J, Olofsson T, Rade J, Fontes M, Porwit-Macdonald A, Behrendtz M, Hoglund M, Johansson B, Fioretos T. 2007. Microarray-based classification of a consecutive series of 121 childhood acute leukemias: Prediction of leukemic and genetic subtype as well as of minimal residual disease status. Leukemia 21:1198–1203.

Arsura M, Mercurio F, Oliver AL, Thorgeirsson SS, Sonenshein GE. 2000. Role of the IkappaB kinase complex in oncogenic Ras- and Raf-mediated transformation of rat liver epithelial cells. Mol Cell Biol 20: 5381–5391.

Barsyte-Lovejoy D, Mao DY, Penn LZ. 2004. c-Myc represses the proximal promoters of GADD45a and GADD153 by a post-RNA polymerase II recruitment mechanism. Oncogene 23:3481–3486.

Belguise K, Guo S, Sonenshein GE. 2007. Activation of FOXO3a by the green tea polyphenol epigallocatechin-3-gallate induces estrogen receptor alpha expression reversing invasive phenotype of breast cancer cells. Cancer Res 67:5763–5770.

Bouchard C, Marquardt J, Bras A, Medema RH, Eilers M. 2004. Myc-induced proliferation and transformation require Akt-mediated phosphorylation of FoxO proteins. EMBO J 23:2830–2840.

Brunet A, Bonni A, Zigmond MJ, Lin MZ, Juo P, Hu LS, Anderson MJ, Arden KC, Blenis J, Greenberg ME. 1999. Akt promotes cell survival by phosphorylating and inhibiting a Forkhead transcription factor. Cell 96:857–868.

Catzavelos C, Bhattacharya N, Ung YC, Wilson JA, Roncari L, Sandhu C, Shaw P, Yeger H, Morava-Protzner I, Kapusta L, Franssen E, Pritchard KI, Slingerland JM. 1997. Decreased levels of the cell-cycle inhibitor p27Kip1 protein: Prognostic implications in primary breast cancer. Nat Med 3:227–230.

Chandramohan V, Jeay S, Pianetti S, Sonenshein GE. 2004. Reciprocal control of Forkhead box O 3a and c-Myc via the phosphatidylinositol 3-kinase pathway coordinately regulates p27Kip1 levels. J Immunol 172:5522–5527.

Chiarle R, Pagano M, Inghirami G. 2001. The cyclin dependent kinase inhibitor p27 and its prognostic role in breast cancer. Breast Cancer Res 3:91–94.

Claassen GF, Hann SR. 2000. A role for transcriptional repression of p21CIP1 by c-Myc in overcoming transforming growth factor beta-induced cell-cycle arrest. Proc Natl Acad Sci USA 97:9498–9503.

Clark KL, Halay ED, Lai E, Burley SK. 1993. Co-crystal structure of the HNF-3/fork head DNA-recognition motif resembles histone H5. Nature 364:412–420.

Dijkers PF, Medema RH, Lammers JW, Koenderman L, Coffer PJ. 2000a. Expression of the pro-apoptotic Bcl-2 family member Bim is regulated by the forkhead transcription factor FKHR-L1. Curr Biol 10:1201–1204.

Dijkers PF, Medema RH, Pals C, Banerji L, Thomas NS, Lam EW, Burgering BM, Raaijmakers JA, Lammers JW, Koenderman L, Coffer PJ. 2000b. Forkhead transcription factor FKHR-L1 modulates cytokine-dependent transcriptional regulation of p27(KIP1). Mol Cell Biol 20: 9138–9148.

Eberhardy SR, D'Cunha CA, Farnham PJ. 2000. Direct examination of histone acetylation on Myc target genes using chromatin immunoprecipitation. J Biol Chem 275:33798–33805.

Erlanson M, Landberg G. 2001. Prognostic implications of p27 and cyclin E protein contents in malignant lymphomas. Leuk Lymphoma 40:461–470.

Ezhevsky SA, Toyoshima H, Hunter T, Scott DW. 1996. Role of cyclin A and p27 in anti-IgM induced G1 growth arrest of murine B-cell lymphomas. Mol Biol Cell 7:553–564.

Feng XH, Liang YY, Liang M, Zhai W, Lin X. 2002. Direct interaction of c-Myc with Smad2 and Smad3 to inhibit TGF-beta-mediated induction of the CDK inhibitor p15(Ink4B). Mol Cell 9:133–143.

FitzGerald MJ, Arsura M, Bellas RE, Yang W, Wu M, Chin L, Mann KK, DePinho RA, Sonenshein GE. 1999. Differential effects of the widely expressed dMax splice variant of Max on E-box vs initiator element-mediated regulation by c-Myc. Oncogene 18:2489–2498.

Furuyama T, Nakazawa T, Nakano I, Mori N. 2000. Identification of the differential distribution patterns of mRNAs and consensus binding sequences for mouse DAF-16 homologues. Biochem J 349:629–634.

Gartel AL, Ye X, Goufman E, Shianov P, Hay N, Najmabadi F, Tyner AL. 2001. Myc represses the p21(WAF1/CIP1) promoter and interacts with Sp1/Sp3. Proc Natl Acad Sci USA 98:4510–4515.

Grumont RJ, Strasser A, Gerondakis S. 2002. B cell growth is controlled by phosphatidylinosotol 3-kinase-dependent induction of Rel/NF-kappaB regulated c-myc transcription. Mol Cell 10:1283–1294.

Hall RK, Yamasaki T, Kucera T, Waltner-Law M, O'Brien R, Granner DK. 2000. Regulation of phosphoenolpyruvate carboxykinase and insulin-like growth factor-binding protein-1 gene expression by insulin. The role of winged helix/forkhead proteins. J Biol Chem 275:30169–30175.

Hu MC, Lee DF, Xia W, Golfman LS, Ou-Yang F, Yang JY, Zou Y, Bao S, Hanada N, Saso H, Kobayashi R, Hung MC. 2004. IkappaB kinase promotes tumorigenesis through inhibition of forkhead FOXO3a. Cell 117:225–237.

Izumi H, Molander C, Penn LZ, Ishisaki A, Kohno K, Funa K. 2001. Mechanism for the transcriptional repression by c-Myc on PDGF beta-receptor. J Cell Sci 114:1533–1544.

Kamesaki H, Nishizawa K, Michaud GY, Cossman J, Kiyono T. 1998. TGF-beta 1 induces the cyclin-dependent kinase inhibitor p27Kip1 mRNA and protein in murine B cells. J Immunol 160:770–777.

Katayose Y, Kim M, Rakkar AN, Li Z, Cowan KH, Seth P. 1997. Promoting apoptosis: A novel activity associated with the cyclin-dependent kinase inhibitor p27. Cancer Res 57:5441–5445.

Kaufmann E, Knochel W. 1996. Five years on the wings of fork head. Mech Dev 57:3–20.

Kiyokawa H, Kineman RD, Manova-Todorova KO, Soares VC, Hoffman ES, Ono M, Khanam D, Hayday AC, Frohman LA, Koff A. 1996. Enhanced growth of mice

lacking the cyclin-dependent kinase inhibitor function of p27(Kip1). Cell 85:721–732.

Kops GJ, Dansen TB, Polderman PE, Saarloos I, Wirtz KW, Coffer PJ, Huang TT, Bos JL, Medema RH, Burgering BM. 2002. Forkhead transcription factor FOXO3a protects quiescent cells from oxidative stress. Nature 419: 316–321.

Lapointe J, Li C, Higgins JP, van de Rijn M, Bair E, Montgomery K, Ferrari M, Egevad L, Rayford W, Bergerheim U, Ekman P, DeMarzo AM, Tibshirani R, Botstein D, Brown PO, Brooks JD, Pollack JR. 2004. Gene expression profiling identifies clinically relevant subtypes of prostate cancer. Proc Natl Acad Sci USA 101: 811–816.

Lee H, Arsura M, Wu M, Duyao M, Buckler AJ, Sonenshein GE. 1995. Role of Rel-related factors in control of c-myc gene transcription in receptor-mediated apoptosis of the murine B cell WEHI 231 line. J Exp Med 181:1169–1177.

Lee LA, Dolde C, Barrett J, Wu CS, Dang CV. 1996. A link between c-Myc-mediated transcriptional repression and neoplastic transformation. J Clin Invest 97:1687–1695.

Li LH, Nerlov C, Prendergast G, MacGregor D, Ziff EB. 1994. c-Myc represses transcription in vivo by a novel mechanism dependent on the initiator element and Myc box II. EMBO J 13:4070–4079.

Lin K, Dorman JB, Rodan A, Kenyon C. 1997. daf-16: An HNF-3/forkhead family member that can function to double the life-span of Caenorhabditis elegans. Science 278:1319–1322.

Loda M, Cukor B, Tam SW, Lavin P, Fiorentino M, Draetta GF, Jessup JM, Pagano M. 1997. Increased proteasome-dependent degradation of the cyclin-dependent kinase inhibitor p27 in aggressive colorectal carcinomas. Nat Med 3:231–234.

Maheswaran S, McCormack JE, Sonenshein GE. 1991. Changes in phosphorylation of myc oncogene and RB antioncogene protein products during growth arrest of the murine lymphoma WEHI 231 cell line. Oncogene 6:1965–1971.

Mao DY, Watson JD, Yan PS, Barsyte-Lovejoy D, Khosravi F, Wong WW, Farnham PJ, Huang TH, Penn LZ. 2003. Analysis of Myc bound loci identified by CpG Island arrays shows that max is essential for Myc-dependent repression. Curr Biol 13:882–886.

Medema RH, Kops GJ, Bos JL, Burgering BM. 2000. AFX-like Forkhead transcription factors mediate cell-cycle regulation by Ras and PKB through p27kip1. Nature 404:782–787.

Nemoto S, Finkel T. 2002. Redox regulation of forkhead proteins through a p66shc-dependent signaling pathway. Science 295:2450–2452.

Ogg S, Paradis S, Gottlieb S, Patterson GI, Lee L, Tissenbaum HA, Ruvkun G. 1997. The Fork head transcription factor DAF-16 transduces insulin-like metabolic and longevity signals in *C. elegans*. Nature 389:994–999.

Paik JH, Kollipara R, Chu G, Ji H, Xiao Y, Ding Z, Miao L, Tothova Z, Horner JW, Carrasco DR, Jiang S, Gilliland DG, Chin L, Wong WH, Castrillon DH, DePinho RA. 2007. FoxOs are lineage-restricted redundant tumor suppressors and regulate endothelial cell homeostasis. Cell 128:309–323.

Polyak K, Lee MH, Erdjument-Bromage H, Koff A, Roberts JM, Tempst P, Massague J. 1994. Cloning of p27Kip1, a cyclin-dependent kinase inhibitor and a potential mediator of extracellular antimitogenic signals. Cell 78:59–66.

Roy AL, Carruthers C, Gutjahr T, Roeder RG. 1993. Direct role for Myc in transcription initiation mediated by interactions with TFII-I. Nature 365:359–361.

Schauer SL, Wang Z, Sonenshein GE, Rothstein TL. 1996. Maintenance of nuclear factor-kappa B/Rel and c-myc expression during CD40 ligand rescue of WEHI 231 early B cells from receptor-mediated apoptosis through modulation of I kappa B proteins. J Immunol 157:81–86.

Schmoll D, Walker KS, Alessi DR, Grempler R, Burchell A, Guo S, Walther R, Unterman TG. 2000. Regulation of glucose-6-phosphatase gene expression by protein kinase Balpha and the forkhead transcription factor FKHR. Evidence for insulin response unit-dependent and -independent effects of insulin on promoter activity. J Biol Chem 275:36324–36333.

Seoane J, Pouponnot C, Staller P, Schader M, Eilers M, Massague J. 2001. TGFbeta influences Myc, Miz-1 and Smad to control the CDK inhibitor p15INK4b. Nat Cell Biol 3:400–408.

Seoane J, Le HV, Shen L, Anderson SA, Massague J. 2004. Integration of Smad and forkhead pathways in the control of neuroepithelial and glioblastoma cell proliferation. Cell 117:211–223.

Staller P, Peukert K, Kiermaier A, Seoane J, Lukas J, Karsunky H, Moroy T, Bartek J, Massague J, Hanel F, Eilers M. 2001. Repression of p15INK4b expression by Myc through association with Miz-1. Nat Cell Biol 3:392–399.

Talbot SG, Estilo C, Maghami E, Sarkaria IS, Pham DK, Oc P, Socci ND, Ngai I, Carlson D, Ghossein R, Viale A, Park BJ, Rusch VW, Singh B. 2005. Gene expression profiling allows distinction between primary and metastatic squamous cell carcinomas in the lung. Cancer Res 65: 3063–3071.

Ticchioni M, Essafi M, Jeandel PY, Davi F, Cassuto JP, Deckert M, Bernard A. 2007. Homeostatic chemokines increase survival of B-chronic lymphocytic leukemia cells through inactivation of transcription factor FOXO3a. Oncogene 26:7081–7091.

Tothova Z, Kollipara R, Huntly BJ, Lee BH, Castrillon DH, Cullen DE, McDowell EP, Lazo-Kallanian S, Williams IR, Sears C, Armstrong SA, Passegue E, DePinho RA, Gilliland DG. 2007. FoxOs are critical mediators of hematopoietic stem cell resistance to physiologic oxidative stress. Cell 128:325–339.

Tran H, Brunet A, Grenier JM, Datta SR, Fornace AJ, Jr., DiStefano PS, Chiang LW, Greenberg ME. 2002. DNA repair pathway stimulated by the forkhead transcription factor FOXO3a through the Gadd45 protein. Science 296: 530–534.

Tsihlias J, Kapusta LR, DeBoer G, Morava-Protzner I, Zbieranowski I, Bhattacharya N, Catzavelos GC, Klotz LH, Slingerland JM. 1998. Loss of cyclin-dependent kinase inhibitor p27Kip1 is a novel prognostic factor in localized human prostate adenocarcinoma. Cancer Res 58:542–548.

Vlach J, Hennecke S, Alevizopoulos K, Conti D, Amati B. 1996. Growth arrest by the cyclin-dependent kinase inhibitor p27Kip1 is abrogated by c-Myc. EMBO J 15: 6595–6604.

Wang X, Gorospe M, Huang Y, Holbrook NJ. 1997. p27Kip1 overexpression causes apoptotic death of mammalian cells. Oncogene 15:2991–2997.

Wu M, Arsura M, Bellas RE, FitzGerald MJ, Lee H, Schauer SL, Sherr DH, Sonenshein GE. 1996. Inhibition of c-myc expression induces apoptosis of WEHI 231 murine B cells. Mol Cell Biol 16:5015–5025.

Wu M, Bellas RE, Shen J, Yang W, Sonenshein GE. 1999. Increased p27Kip1 cyclin-dependent kinase inhibitor gene expression following anti-IgM treatment promotes apoptosis of WEHI 231 B cells. J Immunol 163:6530–6535.

Yang W, Shen J, Wu M, Arsura M, FitzGerald M, Suldan Z, Kim DW, Hofmann CS, Pianetti S, Romieu-Mourez R, Freedman LP, Sonenshein GE. 2001. Repression of transcription of the p27(Kip1) cyclin-dependent kinase inhibitor gene by c-Myc. Oncogene 20:1688–1702.

Yano T, Sander CA, Clark HM, Dolezal MV, Jaffe ES, Raffeld M. 1993. Clustered mutations in the second exon of the MYC gene in sporadic Burkitt's lymphoma. Oncogene 8:2741–2748.